UW Journal of Science and Technology Vol. 5 (2021) 7-11
ISSN: 2523-0123 (Print) 2616-4396 (Online)

University of Wah
Journal of Science and Technology

www.uow.edu.pk

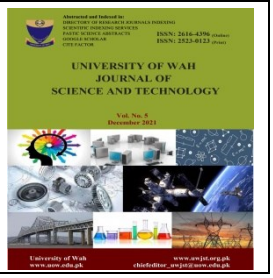

Comparison between ultrathin phonon polariton modes in monolayer hexagonal boron nitrides

[1]Rehan Ali Khan*, [2]Muhammad Imran, [1]Kalimullah and [3]Shah Fahad

***Abstract*—The dispersion properties and characteristics of monolayer hexagonal boron nitrides (*hBN*) supported by transverse magnetic (TM) and transverse electric (TE) phonon polaritons in the air-*hBN*-air structure have been extensively studied. The analytical results show that the *hBN* based TM (TE) phonon polaritons exist in Restsrahlen bands when imaginary surface conductivity is positive (negative). The effective mode indexes of TM phonon polaritons are much higher than those of TE phonon polaritons, with respective values of ~ 3000 and ~ 1.0002 which makes TM more promising in practical realization. In addition, the propagation length of TE polaritons is less lossy and surpasses that of TM polaritons by factor 10^4. This paper compares these important properties and sheds more insight into their applications in photonics and optoelectronic devices.**

Index terms*— *surface phonon polaritons, hexagonal boron nitrides, skin depth, surface conductivity, ultrathin waveguides.

I. Introduction

PHONON polaritons are quasi-particles that result from strong hybridization of light-photons with collective lattice vibration in polar crystals. The representative polar crystal is hexagonal boron nitrides – white graphite, which is a wide band gap semiconductor with interesting optical, mechanical, and electronic properties [1-8]. Similar to fundamental waveguide modes, phonon polaritons in *hBN* exhibit wave-like propagation in fundamental and subsequent high-order modes. This prompts usage of *hBN* in applications such as sensors, nano-imaging, lithography, anomalous refraction/reflection and emitters [9-19]. Restsrahlen bands are two narrow bands in polar crystals where light interacts significantly with the crystals. Longitudinal and transverse optical phonons, abbreviated as LO and TO, separate the bands. Within these bands in one of the alignments of axes (parallel or perpendicular) to the optical axis, the sign of real permittivity shifts to negativ e. The first Restsrahlen band in *hBN* crystals is placed between $21 > f > 24$ THz, whereas the second Restsrahlen band is found between $39 > f > 41$ THz. The out-of-plane real permittivity sign is negative in the first RB, while the in-plane real permittivity sign is negative in the second RB. This demonstrates that the method the flakes are aligned within the crystal impacts the type of light-matter interaction that occurs.

The advent of nanophotonic in two-dimensional materials has broadened the research and integration of two-dimensional based polaritons. Numerous potential proof-of-concept designs and unusual phenomena are possible in the monolayer, few layers, and heterostructures of these exotic materials [12-15]. Plasmon polaritons in metals, semimetals, and semiconductors are the pioneers in the field from the first reported exfoliation of monolayer graphene. Exciton polaritons in the cavity and surface of the transition metal-dicalchogenides (TMD). There is also magnon polaritons in magnetic materials, and cooper pair polaritons in

Manuscript received: September 4,2021; Accepted: December 27, 2021

[1]Department of Electrical Engineering, University of Science and Technology, Bannu, Pakistan.
[2]Institute of Information and Electronic Engineering, Xian Jiaotong University, Xian, China.
[3]College of Electrical Engineering, Zhejiang University, Hangzhou, China.
*Corresponding Author: engr.rehan@ustb.edu.pk

superconducting materials. Hybrid polaritons are extremely significant in numerous potentials such as plasmon-phonons between graphene and *hBN*, plasmon-excitons between graphene and TMD, then possibly phonon-excitons between *hBN* and TMDs.

Unlike bulk polaritons, two-dimensional polaritons are mostly defined based on the sign of imaginary surface conductivity of the ultrathin materials. This facilitates easier characterization of two-dimensional materials, because it can easily be defined in the Maxwell's equation as the surface conducting sheet than the well-known real part of permittivity which is unrealistic in ultrathin materials. When the sign of imaginary surface conductivity is positive, we expect transverse magnetic phonon polaritons within the frequency band, while it is transverse electric phonon polaritons for the negative imaginary surface conductivity [23-27].

In this work, we conceptually analyze the two fundamental phonon polaritons modes in monolayer *hBN*. By numerically comparing these fundamental modes, we found that the TM phonon polaritons exhibit stronger confinement than the weaker confined TE phonon polaritons. The propagation length is intuitively longer in the TE phonon polaritons due to lower losses in TE polaritons. These important comparisons might facilitate greater understanding the properties of the two phonon polaritons modes, which improves their usage in the photonic devices.

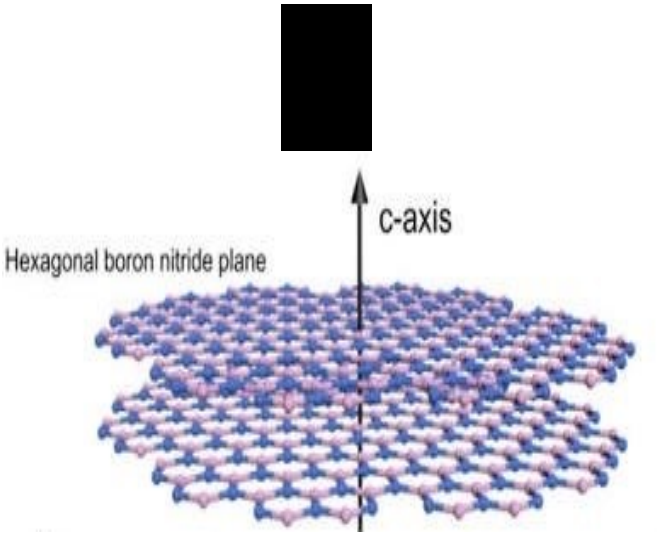

Figure 1: Freestanding monolayer hexagonal boron nitrides diagrams. An air-filled substrate and superstrate surround the monolayer hBN, which is depicted as a surface conducting sheet with surface conductivity.

II. PROPOSED WORK

A. Dispersion relation derivation

First, as shown in Figure 1, we derive the dispersion relation of the TM phonon polaritons. Maxwell's equations are solved for such a system by considering the monolayer placed between two air-filled half spaces. A surface conducting sheet σ_s is regarded to be a monolayer *hBN*. The perpendicular orientation of the crystal was taken into consideration for this work.

As, $\bar{H}_{1y} = A_1 e^{-ik_{1z}z} e^{-k_x x}$, the electromagnetic wave propagates in the x-direction and decays in the normal direction (z-direction), whereas as $\bar{H}_{2y} = A_2 e^{ik_{2z}z} e^{-k_x x}$, the bottom half-space propagates similarly to the higher half-space. Maxwell's equation connection $\bar{E} = \frac{-k \times \bar{H}_y}{\omega \varepsilon_0 \varepsilon_{1,2}}$ may be used to find the appropriate electric field components, where $k = \hat{x}k_x + \hat{y}k_y + \hat{z}k_z$ and ε_0 are the permittivity of free space. The TM SPhP characteristics equation of monolayer *hBN* is found after basic algebraic manipulations as:

$$\frac{k_{1z}}{\varepsilon_1} + \frac{k_{2z}}{\varepsilon_2} - \frac{\sigma_s}{\omega \varepsilon_0} \frac{k_{1z}}{\varepsilon_1} \frac{k_{2z}}{\varepsilon_2} = 0 \ldots\ldots\ldots\ldots\ldots\ldots 1$$

Where $k_{1,2z} = \sqrt{(\varepsilon_{1,2} k_0^2 - k_x^2)}$, $k_0 = \frac{\omega}{c}$, the speed of light in free space is c. The transverse and longitudinal wave vectors are represented by the wave vector components $k_{1,2z}$ and k_x.

Similarly, to derive dispersion relation of the TE SPhP wave, the electric field components are transverse to the propagation direction. For the upper and lower half-spaces can be written as $\bar{E}_{1y} = A_1 e^{-ik_{1z}z} e^{-k_x x}$ and $\bar{E}_{2y} = A_2 e^{ik_{2z}z} e^{-k_x x}$ respectively. The corresponding magnetic field component can be obtained from $\bar{H} = \frac{k \times \bar{E}_y}{\omega \mu_0}$, with μ_0 is the permeability in free space, and the system is considered to be nonmagnetic. Following simple algebraic manipulations, the dispersion relation of TE SPhP is obtained as:

$$k_{z1} + k_{z2} + \sigma_s \omega \mu_0 = 0 \ldots\ldots\ldots\ldots\ldots\ldots 2$$

The effective surface conductivity of an ultrathin *hBN* slab can be calculated as follows from its relative in-plane permittivity $\varepsilon_{r\perp,hBN}(\omega)$ (the component of permittivity perpendicular to the z direction or the optic axis [28,29] of *hBN*):

$$\sigma_s = \left[\varepsilon_{r\perp,hBN}(\omega) - \varepsilon_{r\perp}(\infty)\right] \varepsilon_0 \omega d \ldots\ldots\ldots\ldots 3$$

where $\varepsilon_{r\perp}(\infty) = \lim_{\omega \to \infty} \varepsilon_{r,hBN}(\omega) = 4.87$ [23], and d is the thickness of *hBN*. The relative in-plane permittivity of *hBN* is

given as [16]: $\varepsilon_{r\perp,hBN}(\omega) = \varepsilon_{r\perp}(\infty) + s_v \frac{{\omega^2}_v}{{\omega^2}_v - i\gamma_v\omega - \omega^2}$, where the amplitude decay rate is $\hbar\gamma_v = 0.87$ meV and the normal frequency of vibration $\hbar\omega_v = 170.1$ meV. $s_v = 1.83$ is a dimensionless coupling factor, and $\hbar$ is the reduced Planck's constant.

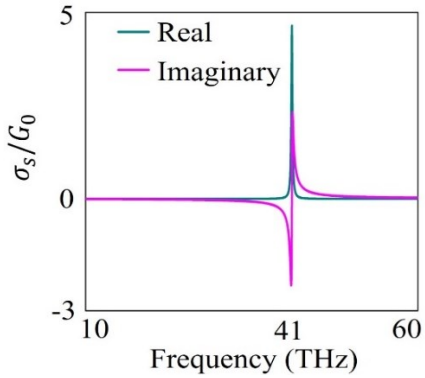

Figure 2: The surface conductivity of monolayer hBN with positive and negative imaginary frequency regions. TM (TE) phonon polaritons can be sustained in the positive (negative) region.

III. RESULTS AND DISCUSSIONS

The frequency areas where the $Im(\sigma_s)$ is positive and negative are our interesting regions for understanding the properties of TM and TE SPhP in monolayer *hBN*. From figure 2, there are two zones with positive and negative imaginary surface conductivity, indicating the possibility of TM and TE SPhP modes within the ultrathin crystal's surface. Figure 2 shows a plot of surface conductivity for both real and imaginary surfaces. The area within the graphic where the $Im(\sigma_s)$ is positive (negative) and approaches zero. Where the magnitude is great, it is natural to expect TM (TE) SPhP to be strongest. These areas, however, are important in regard to our research.

The characteristic equation, which establishes the relationship between the propagation wave vector and the frequency, is the solution to equations 1 and 2. Figure 3 shows the quantity $Re\,(k_x) \times {}^{c}/_{\omega}$, also known as the refractive index, plotted against frequency for both TM (a) and TE (b). The refractive index of TM SPhP can approach ~ 3000, whereas it is ~ 1.0002 for TE SPhP, indicating that the wave is firmly confined for TM significantly more than for TE SPhP.

The ability to tap or utilise electromagnetic energy efficiently is the result; nevertheless, unlike TE polaritons, which are weakly restricted, it can be difficult to distinguish from the light line. This led to the use of TM polaritons in optical communication equipment with significant electromagnetic energy confinement, such as routers, waveguides, and other similar devices. The TE polaritons in *hBN*, however, will soon find a domain in photonic application, according to an intriguing study from [23].

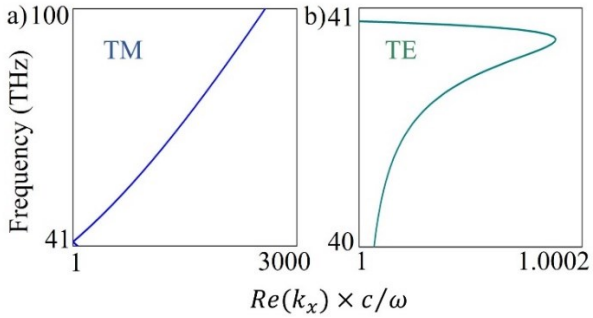

Figure 3: The dispersion relations of the monolayer hBN: a) transverse magnetic b) transverse electric phonon polaritons. The schematics are the same with Figure 1.

The electromagnetic energy's skin-depth (penetration depth) refers to how far the energy enters the crystal. It reveals how far we can employ the crystal in waveguiding, routing, and fibres, among other applications. Skin depth can be expressed as a simple $\delta_{hBN} = 1/Im(k_z)$. Figure 4(a) and Figure 4(b) exhibit numerical plots of dispersive skin-depth for TM and TE, respectively. For TM, the value can be as low as $0.27\lambda_0$ and as high as $5\lambda_0$, whereas for TE, the value can be anywhere in between. Wave penetration performance measures in ultrathin materials are defined by this.

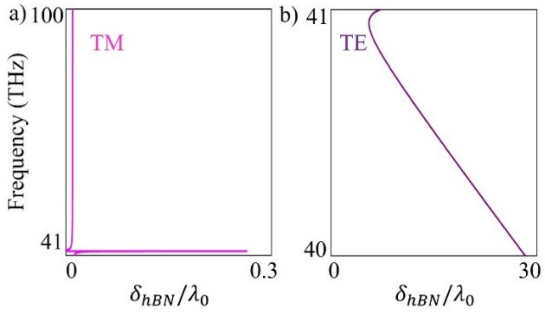

Figure 4: The skin depth of the monolayer hBN: a) TM SPhP, b) TE SPhP. In TM SPhP, the dispersive skin depth can be subwavelength.

The distance that electromagnetic energy travels without attenuation is important in optoelectronic applications. The propagation length is the measurement of this distance. The inverse damping factor $\frac{Re(k_x)}{Imag(k_x)} = 4\pi \frac{L_p}{\lambda_{spp}}$ is the figure of merit used in most photonics analysis to quantify how far the wave travelled. Figure 5 shows the inverse damping factor as a function of frequency for both TM and TE in Figures 5(a) and 5(b). The degree of propagation loss for TM polaritons

increases with frequency, but it is the inverse for TE polaritons. However, because TE polaritons have a longer propagation length, the loss is substantially lower.

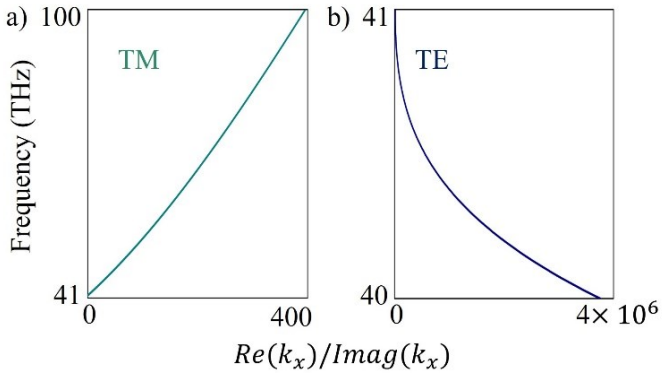

Figure 5: The phonon polaritons' propagation lengths in monolayer hBN: a) TM SPhP, b) TE SPhP.

IV. Conclusion

Comparative analysis has been performed for the TM and TE SPhP in monolayer *hBN*. The system is situated in air-filled half-spaces without considering the effect of the substrate and superstrate. As expected, the well-known TM SPhP exhibits tighter confinement and skin depth, while TE SPhP exhibits lower losses, which makes it a strong candidate for waveguide and routing devices in communication networks. These findings might well place SPhP in monolayer *hBN* as a good choice for optoelectronics, communication, and photonic devices.

References

[1] A. Nagashima, N. Tejima, Y. Gamou, T. Kawai, C. Oshima,
"Electronic Structure of Monolayer Hexagonal Boron Nitride Physisorbed on Metal Surfaces," *Phys. Rev. Lett.* 1995, 75, p 3918−3921, 1995.

[2] K. Watanabe, T. Taniguchi, and H. Kanda, "Direct-bandgap properties and evidence for ultraviolet lasing of hexagonal boron nitride single crystal," *Nat. Mater.* 3, pp. 404–409, 2004.

[3] Y.-N. Xu and W. Y. Ching, "Calculation of ground-state and optical properties of boron nitrides in the hexagonal, cubic, and wurtzite structures," *Phys. Rev. B* 44, pp. 7787–7798,1991.

[4] G. Cassabois, P. Valvin, and B. Gil, "Hexagonal boron nitride is an indirect bandgap semiconductor," *Nat. Photon.* 10, pp. 262–266, 2016.

[5] K.Watanabe, T. Taniguchi, T. Niiyama, K. Miya, and M. Taniguchi, "Far ultraviolet plane-emission handheld device based on hexagonal boron nitride," *Nat. Photon.* 3, pp. 591–594, 2009.

[6] G. Cassabois, P. Valvin, and B. Gil, "Intervalley scattering in hexagonal boron nitride," *Phys. Rev. B* 93, p. 035207, 2016.

[7] K. K. Kim, et al "Synthesis of Monolayer Hexagonal Boron Nitride on Cu Foil Using Chemical Vapor Deposition," *Nano Lett.* 12, p 161−166, 2012.

[8] Y. Liu, S. Bhowmick, B.I. Yakobson, "BN White Graphene with "Colorful" Edges: The Energies and Morphology," *Nano Lett.* 11, p 3113−3116, 2011.

[9] A. Poddubny, I. Iorsh, P. Belov, Y. Kivshar, "Hyperbolic metamaterials" *Nat. Photon*. 7, 948–957, 2013.

[10] T. Low et al "Polaritons in layered two-dimensional materials" *Nat. Materials* 16 pp. 182-194, 2017.

[11] S. Dai et al "Graphene on hexagonal boron nitride as a tunable hyperbolic metamaterial," *Nat. Nanotech.* 10, pp. 682-6, 2015.

[12] D. N. Basov, M. M. Fogler, F. J. García de Abajo, "Polaritons in van der Waals materials," *Science* 354 pp. aag1992, 2016.

[13] J. D. Caldwell, et al "Sub-diffractional volume-confined polaritons in the natural hyperbolic material hexagonal boron nitride," *Nature Commun*. 5, 5221, 2014.

[15] S. Dai, et al "Tunable phonon polaritons in atomically thin van der Waals crystals of boron nitride," *Science* 343, pp. 1125-1129, 2014.

[16] Woessner A et al "Highly confined low-loss plasmons in graphene–boron nitride heterostructures." *Nat. Mater.* 14 pp. 4, 2015.

[17] C. R. Dean, et al "Boron nitride substrates for high-quality graphene electronics," *Nat. Nanotechnol*. 5, pp. 722−726, 2010.

[18] J. Xue, et al "Scanning tunnelling microscopy and spectroscopy of ultra-flat graphene on hexagonal boron nitride," *Nat. Mater*. 10, pp. 282−285, 2011.

[19] G. Shi, "Boron Nitride−Graphene Nanocapacitor and the Origins of Anomalous Size Dependent Increase of Capacitance," *Nano Lett*.14, 1739−1744, 2014.

[23] M. Y. Musa, et al, "Confined transvrese electric phonon polaritons in hexagonal boron nitrides," *2D Materials*, vol. 5, pp. 015018, 2017.

[24] Q. Bao, H. Zhang, B. Wang, Z. Ni, C. H. Y. X. Lim, Y. Wang, D. Y. Tang and K. P. Loh "Broadband graphene polarizer." *Nat. Photonics* 5 411-5, 2011.

[25] G. Shkerdin, H. Alkorre, H. Guoqiang and J. H. Stiens "Modified TE modes of metal waveguide with integrated graphene structure in the sub-terahertz frequency range." *IET Microw. Antennas Propag.* 10 692-9, 2016

[26] L. Sun, Y. Zhang, Y. Wang, C. Zhang, C. Min, Y. Yang, S. Zhu and X. Yuan "Refractive index mapping of single cells

with a graphene-based optical sensor." *Sensors and Actuators B* 242 41-6, 2017.
[27] X. Lin, Y. Shen, I. Kaminer, H. Chen and M. Soljacic "Transverse-electric Brewster effect enabled by nonmagnetic two-dimensional materials." *Phys. Rev. A* 94 023836, 2017.
[28] S. C. Lee, "Crystal orientation dependence of polarized infrared response of sapphire crystal" *Optical Mater.* 37 pp. 773-9, 2014.
[29] S. C. Lee "Surface phonon polaritons responses of hexagonal sapphire crystals with non-polar and semi-polar crystallographic planes" *Optic Lett.* 39 pp. 5467-70, 2014.